UDK 66.017:669.715:620.3
Original scientific article/Izvirni znanstveni članek

ISSN 1580-2949
MTAEC9, 46(6)613(2012)

ALUMINUM-MATRIX NANOCOMPOSITES: SWARM-INTELLIGENCE OPTIMIZATION OF THE MICROSTRUCTURE AND MECHANICAL PROPERTIES

NANOKOMPOZITI NA OSNOVI ALUMINIJA: OPTIMIZACIJA MIKROSTRUKTURE IN MEHANSKIH LASTNOSTI Z UPORABO INTELIGENCE ROJA

Mohsen Ostad Shabani, Ali Mazahery

Karaj Branch, Islamic Azad University, Karaj, Iran
vahid_ostadshabany@yahoo.com

Prejem rokopisa – received: 2012-04-23; sprejem za objavo – accepted for publication: 2012-07-04

In the present research, ceramic nanoparticles were added to the Al-Si aluminum alloy using the casting method. Experimental characterization of the mechanical properties showed that an incorporation of the nanoparticles improved the hardness and strength of the composites. This paper also reports a successful development of an effective approach based on the combination of a parallel particle-swarm optimization and FEM methods to determine the optimum conditions of the Al-matrix nanocomposites in terms of the microstructure and mechanical properties. It has been shown that a parallel particle swarm performs well in the optimization of nanocomposite materials.

Keywords: nanocomposites, Al, optimum conditions

V tej raziskavi so bili dodani keramični nanodelci v zlitino Al-Si z uporabo metode pri ulivanju. Eksperimentalna karakterizacija mehanskih lastnosti je pokazala, da vključitev nanodelcev izboljša trdoto in trdnost kompozitov. Ta članek predstavlja tudi uspešen razvoj učinkovitega približka, ki temelji na kombiniranju teorije vzporednih rojev delcev in FEM-metod, za določanje optimalnih mikrostrukturnih in mehanskih lastnosti nanokompozitov na osnovi aluminija. Pokazalo se je, da je teorija vzporednih rojev delcev učinkovita pri optimiranju nanokompozitnih materialov.

Ključne besede: nanokompoziti, Al, optimalni pogoji

1 INTRODUCTION

Despite a great importance of aluminum alloys as structural materials[1–4], their use in the automotive applications has been limited due to their inferior strength, rigidity and wear resistance, as compared to the ferrous alloys. For many applications it is necessary to improve their mechanical behavior and wear resistance. However, discontinuously-reinforced metal-matrix composites (MMCs) offer a reduced mass, high stiffness and strength, and improved wear resistance. Specifically, the possibility of substituting the iron-based materials with the Al-matrix composites (AMCs) in the automotive components provides a potential for a considerable weight reduction[5,6]. The particle and short-fiber reinforced MMCs have unique and desirable thermal and mechanical properties[7]. When compared to the unreinforced metals and alloys, MMCs have higher strength, Young's modulus[8–10], wear resistance[11], fatigue resistance[12], and lower thermal expansion[13]. They are also relatively inexpensive, compared to their continuous-fiber reinforced counterparts, and can be processed with conventional techniques[14–18].

During the last two decades a lot of research has been focused on AMCs. A wide variety of fabrication techniques have been explored, which include vapor-state methods, liquid-phase methods (infiltration of preforms, rheocasting/thixoforming, melt stirring and squeeze casting) and solid-state methods (powder forming and diffusion bonding)[19–23].

The melt processing, which involves a stirring of ceramic particles into a melt, has a few important advantages including a better matrix-particle bonding, an easier control of the matrix structure, simplicity, low cost of processing, nearer net shape and a wide selection of materials for this fabrication method[19]. A wide range of particle sizes has been used for the reinforcement of MMCs. Normally, the micron-sized particles are used to improve the ultimate tensile and yield strengths of the metal. However, the ductility of MMCs deteriorates significantly with a high ceramic-particle concentration [24,25].

Metal-matrix nanocomposites (MMNCs) are a new class of nanostructured materials, consisting of nano-scale particles used as reinforcements. MMNCs are being considered for many applications because of their improved specific strength, wear resistance, and retained ductility as compared to monolithic alloys[26]. Zhao et al.[27] characterized the properties and deformation behavior of the Al-matrix composites reinforced with the Al_2O_3 nanoparticles. It is reported that the elongation, the ultimate tensile strength and the yield strength of nanocomposites are enhanced with an increase in the

particle-volume fraction, and are markedly higher than that of the Al composites synthesized with the micro-sized particles. Significant developments have been achieved with the nano-SiC/AMCs system processed via the ultrasonic method. The strength of nanocomposites increases with an increase in the volume percentage of the ceramic phase[28,29].

In recent years, some mechanisms were designed to increase the diversity in order to prevent premature convergence to the local minimum. Silva et al. presented a predator-prey model to maintain the population diversity. Zhang proposed to re-initialize the velocities of all the particles at a predefined extinction interval, which simulated the natural process of a mass extinction in the fossil record. Krink proposed several collision strategies to avoid crowding of the swarm. Lovbjerg used self-organized criticality to add diversity[30–38]. In recent years, meta-heuristic algorithms have been applied to a variety of complex problems in order to obtain quality solutions within acceptable computation time. Proposed by Kennedy and Eberhart[39], particle-swarm optimization (PSO) has been drawing attention of many researchers. This algorithm is mostly used to simulate the social behavior of animals such as birds and fish in the nature. Individuals in a flock of birds or a school of fish exchange previous experience and make adjustments accordingly so that they can move toward the objective. The concept is adopted by PSO in searching for optimal solutions.

PSO has been widely applied in many research areas and real-world engineering fields. Examples include task assignment and scheduling, data clustering, power-flow analysis, pattern recognition, roundness-measurement demand forecast, financial decisions, product plans and layout design. It has been demonstrated that PSO performs well in many optimization problems. However, it was observed that the algorithm did not perform well at times. The conversion may be slow when solving complex problems and the search can be occasionally trapped in the local optima. Many attempts have been made to improve the algorithm's efficiency and robustness[40–44].

Although variations of PSO have included different strategies and parameters, all of them follow the same principle of the swarm intelligence. Therefore, all variations show similar features of social behavior. Within a swarm individuals are relatively simple, but their collective behavior becomes quite complex. A group of particles in a swarm move around in a defined search space to find the optimum. Each particle relies on direct and indirect interactions and cooperation with the other particles to determine the next search direction and step size, so the swarm will move around and gradually converge toward the candidates of the global optima or the local optima. Thus, the center of the swarm is probably near the optimum[35–44]. While this position changes during the search process, it can supply very useful information for capturing the optimum.

In comparison with microcomposites, the research on nanocomposites is still limited. The key reason is perhaps related to the difficulty in synthesizing these composites due to their high viscosity, poor wettability of the nanoparticles in the metal matrix, and a large surface-to-volume ratio.

Therefore, the present study aims at the development of the stir-casting process required for producing nanomatrix composites and investigating the PSO performance with respect to the microstructure and mechanical properties of the nano-Al_2O_3-reinforced A356-alloy-matrix composites.

2 EXPERIMENTAL PROCEDURE

Nano-Al_2O_3 particles were used as reinforcement with an average particle size of 50 nm and the chemical composition that is listed in **Table 1**. The aluminum alloy A356 was used as the matrix material due to its good castability. The chemical composition of A356 is included in **Table 2**. In order to improve the wettability of the particles, 1 % of Mg was added to the original composition of A356. The Al_2O_3-particle reinforcement is characterized by its good thermal stability, high hardness and wear resistance. In addition, nano-Al_2O_3 particles were chosen because, up to now, Al_2O_3 is one of the most commonly used particle reinforcements in Al MMCs due to its low cost and availability. The metal-matrix composites reinforced with volume fractions (0.5, 1, 1.5, 2, 2.5 ... 5) % of Al_2O_3 have been produced by using a vortex method. A detailed description of the nanocomposite processing was discussed in the previous work[45]. Composite slurry was step cast into a CO_2-sand mould. The microstructure was investigated with optical microscopy (Prior N334) and transmission electron microscopy (TEM, Philips CM20T, 200 kV, EDX). The amount of the porosity in the cast alloy and in the composite was determined by comparing the measured density with their theoretical density. The compression and tension tests were used to assess the mechanical behavior of the composites.

Table 1: Chemical composition of alumina
Tabela 1: Kemijska sestava aluminijevega oksida

Other magnetic materials	CaO	TiO_2	Fe_2O_3	α-Alumina	Element
0.02	1.1	1.8	0.8	93	*w*/%

Table 2: Chemical composition of A356
Tabela 2: Kemijska sestava A356

Ni	Ti	Zn	Mn	Mg	Cu	Fe	Si	Al	Element
0.05	0.01	0.02	0.02	0.38	0.001	0.10	7.5	Balance	*w*/%

3 PARALLEL PSO

PSO was first introduced by Kennedy and Eberhart[39]. The algorithm is driven by the social behavior of a bird flock and can be viewed as a population-based stochastic optimization algorithm. In PSO, the group is a community composed of individuals called particles, and all the particles fly around in a multidimensional search space. Each particle adjusts its own "flight path" according to its flying experience as well as the flying experience of the neighboring particles. This process can be generally described with a group of vectors denoted as X_i, V_i, P_i. Let x and v denote a particle's position and velocity in a search space. The ith particle can be represented as $X_i = (x_{i1}, x_{i2} \ldots x_{iD})$ in the D-dimensional search space. The best previous position of the ith particle is recorded and represented as $P_i = (p_{i1}, p_{i2} \ldots p_{iD})$ ($i = 1, 2 \ldots m$). The index of the best particle in the group, i.e., the particle with the smallest function value, is represented by $P_g = (p_{g1}, p_{g2} \ldots p_{gD})$, while the velocity of the ith particle is represented by $V_i = (v_{i1}, v_{i2} \ldots v_{iD})$. According to Bratton and Kennedy, the modified velocity and position of each particle can be manipulated according to the following equations:

$$X^i_{k+1} = V^i_{k+1} + X^i_k \quad (1)$$

$$V^i_{k+1} = w_k V^i_k + c_1 r_1 (p^i_k - X^i_k) + c_2 r_2 (p^g_k - X^i_k) \quad (2)$$

where c_1 and c_2 are positive constants known as acceleration coefficients; X is the constriction factor that controls the velocity's magnitude; r_1 and r_2 are the two random numbers within the range [0, 1]; and w is the inertia factor that linearly decreases from 0.9 to 0.4 throughout the search process. In addition, the velocities of the particles are confined within $[V_{min}, V_{max}]^D$. If a velocity element exceeds the threshold V_{min} or V_{max}, it is set equal to the corresponding threshold.

Although several modifications to the original swarm algorithm have been made to improve its performance and adapt it to specific types of problems, the parallel version has not been previously implemented.

3.1 Concurrent Operation and Scalability

The algorithm should operate in such a way that it can be easily decomposed for a parallel operation on a multi-processor machine. Furthermore, it is highly desirable that it is scalable. This implies that the nature of the algorithm should not place a limit on the amount of the computational nodes that can be utilized[39–44].

3.2 Coherence

Parallelization should have no adverse affect on the algorithm's operation. Calculations sensitive to the program order should appear to have occurred in exactly the same order as in the original formulation, leading to the exact same final answer as obtained by a serial implementation[38–42].

3.3 Optimization

1. Evaluate all i particle-fitness values f_i^k in parallel using design-space coordinates $x_i{}^k$.
2. Perform barrier synchronization of all fitness-evaluation results.
3. If $f_i^k \leq f_i{}^{best}$ then $f_i^{best} = f_i^k$, $p_i^k = x_i^k$.
4. If $f_i^k \leq f_g^{best}$ then $f_g^{best} = f_i^k$, $p_g{}^k = x_i^k$.
5. Update all particle velocities v_i^k for $i = 1, \ldots, p$.
6. Update all particle positions x_i^k for $i = 1, \ldots, p$.
7. Increment k.

The best ever fitness value of a particle at the design coordinates p_i^k is denoted by f_i^{best} and the best ever fitness value of the overall swarm at the coordinates $p_g{}^k$ is denoted by $f_g{}^{best}$. At the initialization time step $k = 0$, the particle velocities $v_0{}^i$ are initialized to random values within the limits $0 \leq v_0 \leq v_0{}^{max}$. The vector $v_0{}^{max}$ is calculated as a fraction of the distance between the upper and lower bounds.

4 NETWORK COMMUNICATION

In a parallel computational environment, the main performance bottleneck is the communication latency between the processors[6]. This is especially true for large clusters of computers where the use of high-performance network interfaces is limited due to their high costs. To keep the communication between different computational nodes at a minimum, the fitness-evaluation tasks are used as the level of granularity for the parallel software[46]. As previously mentioned each of these evaluations can be performed independently and requires no communication, aside from receiving design-space coordinates, for evaluating and reporting the fitness value at the end of the analysis[2].

The optimization infrastructure is organized into a coordinating node and several computational nodes. The PSO algorithm functions and task orchestration are performed by the coordinating node, which assigns the design coordinates to be evaluated, in parallel, to the computational nodes. With this approach, no communication is required between the computational nodes as individual design-fitness evaluations are independent of each other. The only necessary communication is between the coordinating node and the computational nodes encompassing the following:

- Several distinct, design-variable, configuration vectors assigned by the coordinating node to slave nodes for fitness evaluation.
- Fitness values reported from slave nodes to the coordinating node.
- Synchronization signals to maintain program coherence.
- Termination signals from the coordinating node to slave nodes on the completion of the analysis in order for the program to stop cleanly.

Figure 1 shows the flowchart of the parallel PSO model that was used in this investigation. The procedure of the parallel PSO is:

Step 1. Initialization
Step 1.1. initialize the population size Pop-Size, inertia weight w, acceleration factors c_1 and c_2
Step 1.2. initialize all particles X^i_k and V^i_k
Step 1.3. evaluate $f(X_n)$ over all particles
Step 1.4. identify the p_{best} for each particle and g_{best} for all particles
Step 2. Iteration
Step 2.1. update the velocity V^i_{k+1} according to Eq. (2)
Step 2.2. update the position X^i_{k+1} according to Eq. (1)
Step 2.3. update p_{best} and g_{best}
Step 2.4. implement the parallel PSO strategy on the g_{best} particle
Step 3. if the stopping criterion is met, output the best solution g_{best} found so far; otherwise, go to Step 2

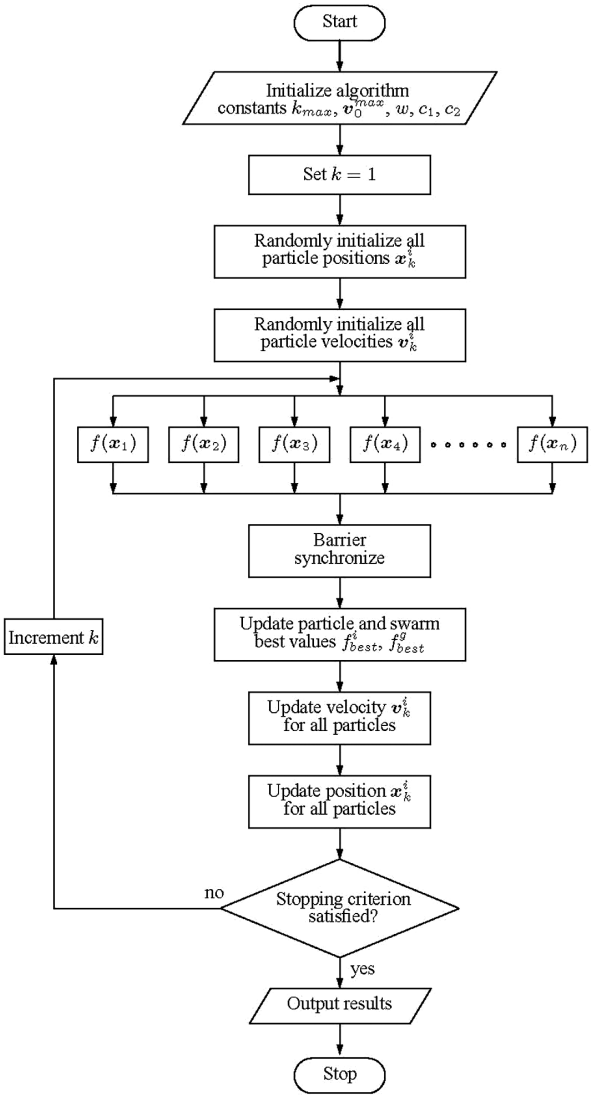

Figure 1: Flowchart of the parallel PSO model
Slika 1: Potek vzporednega PSO-modela

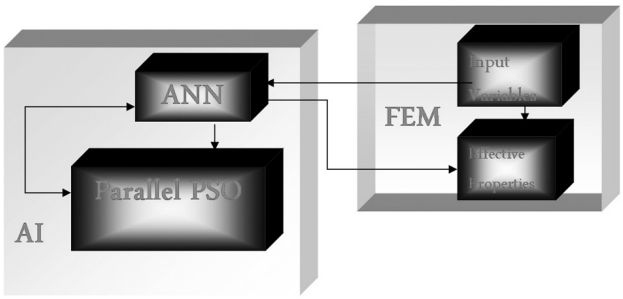

Figure 2: Flowchart of the combined FEM-Parallel PSO -ANN model
Slika 2: Potek kombiniranega FEM-Parallel PSO-ANN-modela

The finite-element method (FEM) was used for discretization. Based on the transient temperature[2], FEM is used to calculate the cooling rate and the temperature gradient. **Figure 2** shows the flowchart of the combined FEM-Parallel PSO-ANN model that was used in this investigation.

5 RESULTS AND DISCUSSION

Because of the casting process, the nanoparticles are anticipated to be distributed between the dendrite branches, leaving the dendrite branches as particle-free regions in the material. **Figure 3** shows an optical micrograph of the composite samples containing the volume fraction 5 % of the nanosized Al_2O_3 particles. As expected, α-aluminums are predominately present in the as-cast A356-matrix composite. Composite samples show higher hardness and UTS than their unreinforced counterparts (**Figure 4**). The higher hardness and UTS of the composites demonstrate the fact that Al_2O_3 particles are incorporated into the Al matrix and act as obstacles to the motion of dislocation. The composite samples were subjected to TEM investigations, with a particular focus on the presence of nanoparticles (**Figure 5**). The TEM micrograph of the composite also confirmed a uniform dispersion of nanoparticles in the Al matrix. It is

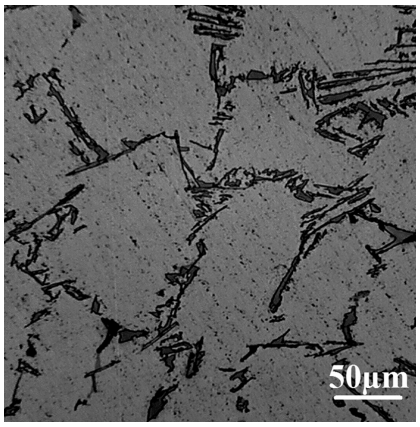

Figure 3: Optical micrograph of Al nanocomposites reinforced with the volume fraction of Al_2O_3 5 %
Slika 3: Svetlobni mikroposnetek Al nanokompozita, utrjenega z volumenskim deležem Al_2O_3 5 %

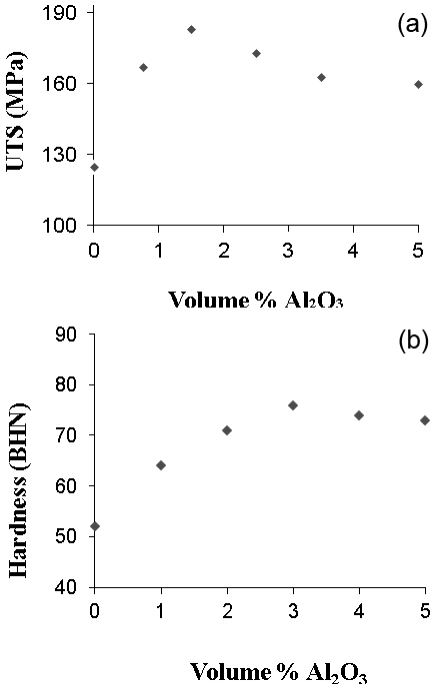

Figure 4: Variations of mechanical properties as functions of volume fractions nano-Al_2O_3 particulates: a) UTS, b) hardness

Slika 4: Spreminjanje mehanskih lastnosti v odvisnosti od volumenskega deleža nano-Al_2O_3 delcev: a) natezna trdnost, b) trdota

indicated that the UTS of the alloy primarily increases with an addition of nano-Al_2O_3. The tensile-strength increment can be attributed to the reduced grain size. It is reported that an introduction of particles into the particle-free matrices provides some heterogeneous nucleation sites during the solidification, resulting in a more refined microstructure (**Table 3**)[26,45]. The improvement in ductility is consistent with the findings of Hassan and Gupta[46–48] who had observed an improved ductility caused by a grain refinement and slip on the extra non-basal planes. The enhancement in the values observed in the tensile strength of these composites, in

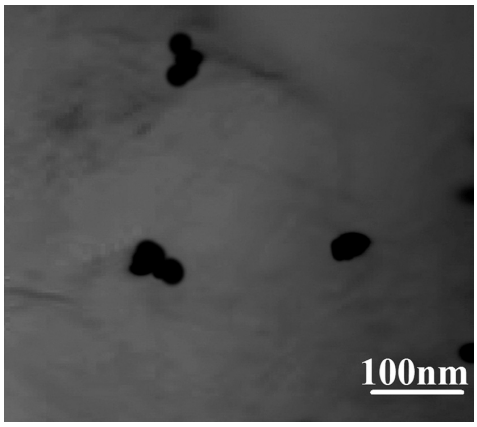

Figure 5: TEM micrograph of Al nanocomposites reinforced with the volume fraction of Al_2O_3 3 %

Slika 5: TEM-posnetek Al nanokompozita, ojačanega z volumenskim deležem Al_2O_3 3 %

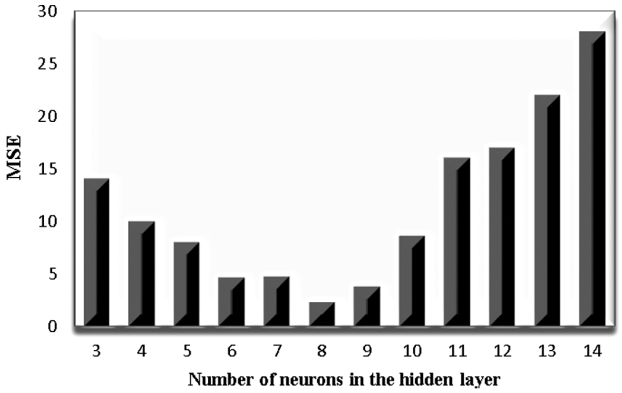

Figure 6: Effect of the number of neurons in the hidden layer on the network performance

Slika 6: Učinek števila nevronov v skritem sloju na zmogljivost mreže

comparison to monolithic aluminium, can also be ascribed to the strong multidirectional thermal stress at the Al/Al_2O_3 interface. It is reported by the other investigators that a low degree of porosity leads to an effective transfer of an applied tensile load to the uniformly distributed, strong Al_2O_3 particulates. **Table 3** indicates that the density of both the unreinforced alloy and composites are close to their theoretical density.

Table 3: Mechanical and microstructural properties as functions of volume percentage of nano-Al_2O_3 particles

Tabela 3: Mehanske lastnosti in značilnosti mikrostrukture v odvisnosti od volumenskega deleža nano Al_2O_3-delcev, φ/%

Al_2O_3 φ/%	Porosity φ/%	Grain size (μm)	Elongation (%)
Un-reinforced	0.47	44	3
0.75	0.77	35	1.9
1.5	1.1	31	1.78
2.5	1.4	27	1.9
3.5	1.75	25	1.8
5	2.3	24	1.75

Artificial neural network (ANN) models were then used to predict and simulate the correlations between the solidification and working conditions as well as mechanical properties. There is no known concept about the selection of the number of neurons in the hidden layer. The neuron number in the hidden layer can be found experimentally[2]. The results of this investigation show that the ANN consisted of three layers – input, hidden and output layers – similar to **Figure 6**, with 8 nodes in the hidden layer and the lowest mean-square error (MSE), and could be used as the fitness function in the particle-swarm optimization. The original PSO algorithm was implemented with a synchronized scheme for updating the best "remembered" individual and group fitness values, f_i^k and f_g^k, and their associated positions p_i^k and p_g^k. This entails performing the fitness evaluations for the entire swarm before updating the best fitness values[43]. The subsequent experimentation revealed that the improved convergence rates can be obtained by

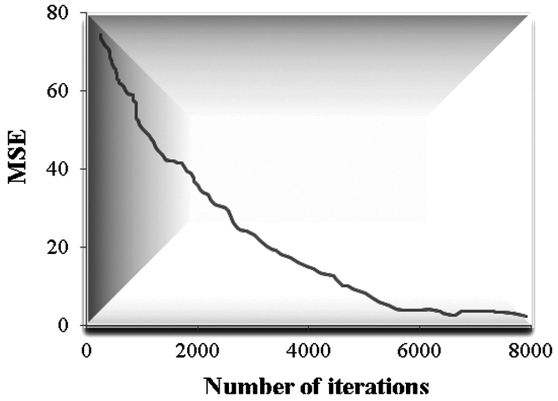

Figure 7: Effect of the iteration number on MSE
Slika 7: Vpliv števila ponovitev na MSE

updating the f_i^k and f_g^k values and their positions after each individual fitness evaluation. It is speculated that because the updating occurs immediately after each fitness evaluation, the swarm reacts more quickly to an improvement in the best-found fitness value. With the parallel implementation, however, this asynchronous improvement on the swarm is lost since the fitness evaluations are performed concurrently. The parallel algorithm requires updating f_i^k and f_g^k for the entire swarm after all fitness evaluations have been performed, as in the original particle-swarm formulation. Consequently, the swarm will react more slowly to the changes of the best fitness-value "position" in the design space. This produces an unavoidable performance loss in terms of convergence rate compared to the asynchronous implementation and can be considered as part of the overhead associated with the parallelization.

The swarm is composed of the particles, where each particle represents a possible solution to an optimization problem. A particle will explore the search area on the basis of two components: its personal experience and the collective experience of the swarm. The swarm tries to maximize the value of the objective function. The "particles" for the PSO are mathematical constructs, having three main parameters: position, velocity and fitness. Position represents the unknown variables of the problem, velocity determines the rate of change of the position, and fitness is a measure of how well a particle solves the optimization problem.

The objective function is a measure of the quality of a solution. The swarm attempts to maximize (or minimize) the objective function. The fitness of a particle is the value of the objective function at the particle's position. The objective functions used in this study are porosity, UTS, grain size and hardness.

Figure 7 shows the effect of an iteration number on MSE of a developed ANN. The number of iterations was selected to be 8000. The final, optimized Al-matrix-nanocomposite process parameters were 1.83 % of Al_2O_3 nanoparticles, 10 °C/s cooling rate, 100000 °C/m temperature gradient, 1.12 % porosity, 184.14 UTS, 30.28 μm grain size and 72.89 BHN hardness. Therefore, the parallel particle-swarm optimization gives the optimal process conditions for an Al matrix reinforced with the nano-Al_2O_3 particulates.

6 CONCLUSION

In this research, a novel particle-swarm optimization is presented, including the design concept as well as the detailed procedure. In this algorithm, the parameter setting and the mechanism of the selective particle regeneration are proposed. There is no obvious effect of the nanoparticle content on the ductility of the composites. In contrast to the plasticity, the composites' strength and hardness are clearly influenced by the effect of the volume fraction of nano-Al_2O_3. The application of the PSO in this work is aimed at minimizing the porosity and the grain size and maximizing the mechanical properties of Al-matrix nanocomposites.

7 REFERENCES

[1] L. Ceschini, A. Morri, G. Sambogna, J. Mater. Process. Technol., 204 (**2008**), 231–238
[2] M. O. Shabani, A. Mazahery, Mater. Tehnol., 46 (**2012**) 2, 81–85
[3] E. de Freitas, M. Ferrante, C. T. Ruckert, W. W. Bose Filho, Mat. Sci. Eng., A 479 (**2008**), 171–180
[4] M. O. Shabani, A. Mazahery, Appl. Math. Model., 35 (**2011**), 5707–5713
[5] R. G. Reddy, Rev. Adv. Mater. Sci., 5 (**2003**), 121
[6] A. Mazahery, M. O. Shabani, Composites: Part B, 43 (**2012**), 1302–1308
[7] N. Chawla, K. K. Chawla, Metal Matrix Composites, Springer, New York 2006
[8] M. J. Koczak, S. C. Khatri, J. E. Allison, M. G. Bader. In: S. Suresh, A. Mortensen, A. Needleman (Eds.), Fundamentals of Metal Matrix Composites, Butterworth-Heinemann, Boston, MA 1993
[9] S. Elomari, R. Boukhili, M. D. Skibo, J. Mater. Sci., 30 (**1995**), 3037
[10] J. N. Fridlyander (Ed.), Metal Matrix Composites, Chapman and Hall, Oxford 1995
[11] F. A. Girot, J. M. Quenisset, R. Nashlain, Compos. Sci. Technol., 30 (**1987**), 155
[12] R. H. Jones, C. A. Lavender, M. T. Smith, Scripta Metall., 21 (**1987**), 1565
[13] Duralcan Composites Casting Guidelines, Duralcan Composites: Mechanical and Physical Property, Wrought Composites, SI Units, Duralcan USA, San Diego, CA 1992
[14] A. Mazahery, M. O. Shabani, Ceram. Int., 38 (**2012**), 1887–1895
[15] J. Sadanandam, G. Bhikshamaiah, M. K. Jain, J. Mater. Sci. Lett., 11 (**1992**), 1518
[16] M. Okumura, Y. Koyo, T. Ito, K. Yoshizaki, H. Yamashita, T. Fujiwara, Proc. Int. SAMPE Electron. Conf., 6 (**1992**), 285
[17] A. Mazahery, M. O. Shabani, Ceram. Int., 38 (**2012**), 4263–4269
[18] C. Zweben, JOM, 44 (**1992**), 15
[19] M. O. Shabani, A. Mazahery, M. R. Rahimipour, M. Razavi, J. King Saud Univ. Eng. Sci., 24 (**2012**), 107–113
[20] D. B. Miracle, Compos. Sci. Technol., 65 (**2005**), 2526–2540
[21] B. Ralph, W. B. Lee, J. Mater. Process. Technol., 63 (**1997**), 339–353
[22] W. C. Harrigan, Mater Sci. Eng., A 244 (**1998**), 75–79
[23] H. P. Degischer, Mater. Des., 18 (**1997**) 4–6, 221–226
[24] Y. C. Kang, S. L. I. Chen, Chem. Phys., 85 (**2004**) 2–3, 438–443

[25] E. M. Maik, O. Beort, S. Kleiner, U. Vogt, Compos. Sci. Technol., 679 (**2007**), 2377–2383
[26] M. Habibnejad - Korayema, R. Mahmudi, W. J. Pooleb, Mater. Sci. Eng., A 519 (**2009**), 198–203
[27] Y. T. Zhao, S. L. Zhang, G. Chen, X. N. Cheng, C. Q. Wang, Compos. Sci. Technol., 68 (**2008**), 1463–1470
[28] J. Lan, Y. Yang, X. Li, Mater. Sci. Eng., A 386 (**2004**), 284–290
[29] J. Lan, Y. Yang, X. Li, Mater. Sci. Eng., A 380 (**2004**), 378–383
[30] M. O. Shabani, A. Mazahery, JOM, 63 (**2011**), 132–316
[31] A. N. Sadigh, M. Mozafari, B. Karimi, Advances in Engineering Software, 45 (**2012**), 144–152
[32] A. Kaveh, S. Talatahari, Computers and Structures, 88 (**2010**), 1220–1229
[33] S. Talatahari, B. Farahmand Azar, R. Sheikholeslami, A. H. Gandomi, Commun Nonlinear Sci Numer Simulat, 17 (**2012**), 1312–1319
[34] M. O. Shabani, A. Mazahery, P. Davami, N.Varahram, Kovove Mater., 49 (**2011**), 253–258
[35] C. Tsai, I. Kao, Expert Sys. with Appl., 38 (**2011**), 6565–6576
[36] L. Zhao, F. Qian, Y. Yang, Y. Zeng, H. Su, Applied Soft Computing, 10 (**2010**), 938–944
[37] A. Mazahery, M. O. Shabani, Powder Technol., 217 (**2012**), 558–565
[38] J. Kennedy, R. C. Eberhart, Particle swarm optimization, Proceedings of the 1995 IEEE International Conference on Neural Networks, 4 (**1995**), 1942–1948
[39] J. Kennedy, R. Mendes, Proceedings of the Congress on Evolutionary Computation, 2002, 1671–1676
[40] A. Safari, R. Jahani, H. A. Shayanfar, J. Olamaei, International Journal of Electrical and Electronics Engineering, 4 (**2010**) 8, 550–553
[41] H. Yoshida, K. Kawata, Y. Fukuyama, IEEE Transactions on Power Systems, 15 (**2000**), 1232–1239
[42] B. Monien, F. Ramme, H. Salmen, Proceedings of the 3rd International Symposium of Graph Drawing, Springer-Verlag, Berlin, 1995, 396–408
[43] G. Celli, E. Ghiani, S. Mocci, F. Pilo, IEEE Transactions on Power Systems, 20 (**2005**) 2, 750–757
[44] J. J. Liang, A. K. Qin, P. N. Suganthan, S. Baskar, Proceedings of IEEE Conference on Systems, Man and Cybernetics, 2004, 3659–3664
[45] A. Mazahery, M. O. Shabani, J. Compos. Mater., 45 (**2011**), 2579–2586
[46] M. O. Shabani, A. Mazahery, JOM, 64 (**2012**), 323– 329
[47] S. F. Hassan, M. Gupta, J. Mater. Sci., 41 (**2006**), 2229–2236
[48] S. F. Hassan, M. Gupta, Mater. Sci. Eng., A 392 (**2005**), 163–168